Hindawi
Mathematical Problems in Engineering
Volume 2021, Article ID 9994573, 13 pages
https://doi.org/10.1155/2021/9994573

*Research Article*

# Epipolar Multitarget Velocity Probability Data Association Algorithm Based on the Movement Characteristics of Blasting Fragments

**Jinyang Chen**,[1,2] **Shangjiang Yu**,[2] **Xian Chen**,[2] **Yongjun Zhao**,[1] **Yunhe Cao**,[3] **and Sheng Wang**[1]

[1]*PLA Strategic Support Force Information Engineering University, Zhengzhou 450001, Henan, China*
[2]*Research Institute for National Defense Engineering of Academy of Military Science PLA, Luoyang 471023, Henan, China*
[3]*Xidian University, Xi'an 710071, Shanxi, China*

Correspondence should be addressed to Jinyang Chen; jinyang870210@163.com and Yunhe Cao; cyh_xidian@163.com

Received 11 March 2021; Accepted 12 August 2021; Published 6 September 2021

Academic Editor: Xiaoheng Chang



Fragments generated from the blast-fragmentation warhead after blasting are typically multiple, fast, small, and dense. In light of the epipolar multitarget feature of blasting fragments, this paper utilizes the movement characteristics of blasting fragments for modeling. Then, the modeling results are adopted in probabilistic data association (PDA) algorithm of multitarget tracking. A novel epipolar multitarget velocity PDA (VPDA) algorithm is proposed based on the movement characteristics of blasting fragments. This algorithm forms the movement characteristics with the finite element simulation results of warhead blasting fragments, utilizes the Doppler velocity probability to reassign the association probability, and updates the state and covariance of each target through the probability weighted fusion. Simulation results demonstrate that, the computational complexity of the proposed algorithm is close to that of PDA algorithm, and the association success rate and the state value update error approximates to the association effects of joint probabilistic data association (JPDA) algorithm, which can effectively track the fragments with identical velocity while reducing the complexity of the epipolar multitarget tracking algorithm, and can respond to the group target tracking scenario.

## 1. Introduction

The fragment is a sort of typical destruction pattern of weapon warhead. During the development and customization process of blast-fragmentation warhead, it is required to test the fragment group velocity, fragment size, angle and field of fragment dispersion, velocity attenuation and spatial distribution. However, the small field range, great environmental impact factor, failure of obtaining the overall distribution laws of fragments, and many other problems [1–3], exist in traditional test methods. When the warhead fragment test is performed with the array-based radar imaging method, the radar cross section (RCS) property is relatively obvious, because all fragments are metal materials. After the fragment test data are obtained with the array-based radar imaging method, it is possible to obtain the spatial position results of fragments at different time with the conventional radar signal processing method [4]. However, a huge challenge appears in data processing due to the great number of blasting fragments.

The fragmentation warhead is generally divided into prefabricated fragmentation warhead, semi-prefabricated fragmentation warhead and natural fragmentation warhead. The fragmentation dispersion law of prefabricated fragmentation warhead and semi-prefabricated fragmentation warhead is related to the characteristics of prefabrication, the design is in good agreement with the actual distribution after the final explosion, and the fragmentation scattering characteristics of the natural fragmentation warhead are more random [5]. For the radar used in this paper, the

performance and resolution of the natural fragmentation warhead and the radar are matched, so the target of this paper is the natural fragmentation warhead.

Fragments generated from the blast-fragmentation warhead after blasting are typically multiple, fast, small and dense. More specifically, the number of fragments is thousands, even tens of thousands. Fast means the speed of fragments is generally 300–2500 m/s. Small means the size of fragments and RCS are small, generally the RCS of fragments is less than −40 dbm. Dense means that multiple fragments move together and the distance between fragments could be very small, which brings a great challenge to the measurement of the motion characteristics of fragments [6].

As to the processing methods of fragment group target data, multitarget association and tracking theory is usually adopted. These methods can implement plot-to-track association, generate flight trajectory, and further analyze the initial velocity of target and its distribution, velocity attenuation, density, placement spread and other movement properties. During this process, the multitarget tracking is most critical. The association and management of multitarget flight trajectory include the start, keeping and disappearance of the flight trajectory [7]. Classical trajectory association and management algorithms include the nearest neighbor algorithm, probabilistic data association (PDA) algorithm, and multiple hypothesis tracking (MHT). They have the common defects, namely, it is impossible to adapt to dense multiple targets as well as tracking scenarios with continuously varying target quantity [8]. Consequently, these methods could not be used in fragment tracking.

In dense clutter environment, the PDA algorithm [9] may avoid the error tracking problem easily occurring to the nearest neighbor method. Therefore, it has the advantage of minimum computational complexity, but it is only applicable to single-target data association processing or multitarget scenarios without any track-crossing. When track-crossing or close track distance appears in multitarget tracking scenario, the PDA algorithm may cause incorrect estimation of target state, because it does not consider the measurement value attribution problem in the crossing gate [10]. In this respect, the well-known joint probabilistic data association (JPDA) algorithm is proposed in [11]. JPDA algorithm calculates the correlation probability between observation data and each target, and thus has much better performance in multitarget data association [12]. However, its computational complexity focuses on the computation of joint event probability. When the number of targets and measurement values increase, the quantity of association matrices divided by matrix confirmation will greatly increase. Therefore, the huge computational complexity of JPDA algorithm makes it unacceptable in practical applications [13, 14].

In this paper, we fully consider the movement features of blasting fragments. A novel epipolar multitarget velocity PDA (VPDA) algorithm is proposed, which utilizes the Doppler velocity probability to reassign the association probability, and updates the state and covariance of each target through the probability weighted fusion. Simulation results demonstrate that the proposed algorithm achieves satisfactory tracking performance but has much lower computational complexity.

## 2. Movement Characteristics Model of Warhead Blasting Fragments

Due to the very high costs of warhead blasting test, it is unrealistic to obtain the complete movement characteristics of warhead fragments after the blasting through the true blasting test method. As a result, it is the commonly used method within the modern military field to carry out the modeling and simulation for the ammunition blasting process, and further obtain the weapon performance parameters. In addition, as the mainstream technology of computer simulation at present, the finite element simulation may handle various complex physics scenarios and have excellent interaction function upon the simulation of physics process similar to warhead blasting. Therefore, the combined use is adopted. For instance, in literature [15], the finite element simulation technology is used to establish the fluid-solid interaction model, the detonation driving process of the fully prefabricated fragment antipersonnel warhead is simulated, and the relationship between the dispersion angle range and dispersion angle is obtained; in literature [16], the finite element modeling is conducted for the ship-to-air missile warhead, the analytical model of fragment dispersion movement laws is established, and the fragment dispersion initial direction angle theory is studied; in literature [17], the finite element analysis is made for the dispersion conditions of prefabricated fragments in four shapes, the dispersion velocity of fragments is compared, and the optimal method of improving the combat destruction performance of the warhead is obtained. Therefore, this paper simulates the movement process of warhead fragments after the blasting through the finite element simulation technology. Accordingly, the movement conditions of fragments under the static/dynamic blasting conditions of the warhead are analyzed and used as the input evidence of multifragment target tracking.

In general blasting scenarios, the fragments of axial symmetric rotational warhead mainly have two dispersion patterns, namely, static dispersion and dynamic dispersion. Among them, the former refers to the fragment dispersion generated from the blasting of warhead under the static state, and the latter refers to the fragment dispersion generated from the blasting of warhead under the movement state. The fragment dispersion patterns for various typical shapes of warhead at static blasting are as shown in Figure 1.

After the common axial symmetric fragment warhead is detonated under the static state, the fragment density is symmetrically distributed around the center of a circle on the equatorial plane of fragment warhead, and it is unevenly distributed on the epipolar plane, as shown in Figure 2.

As shown in Figure 2, about 10% fragments of the total count are scattered at both ends of the fragment warhead and the remaining fragments are scattered within the range nearby the middle part of the warhead.

In order to obtain the relationship between the remaining velocity of the fragment and time, the instant

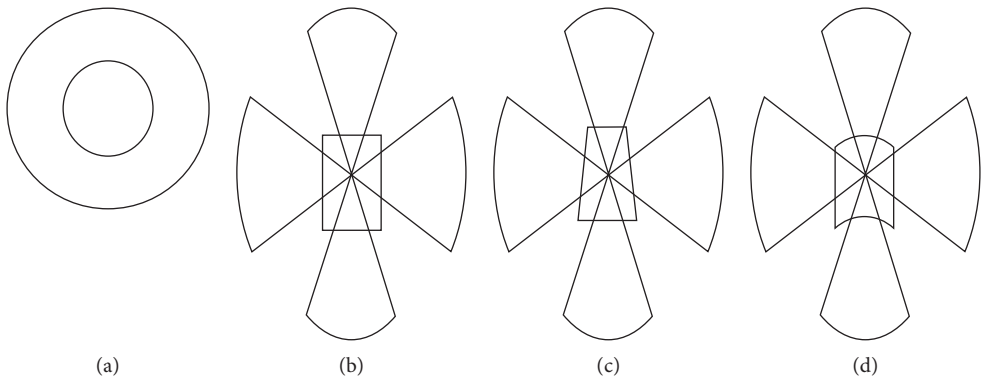


Figure 1: Static blasting dispersion patterns of warhead fragments. (a) Sphere. (b) Cylinder. (c) Truncated cone shape. (d) Circular arc.

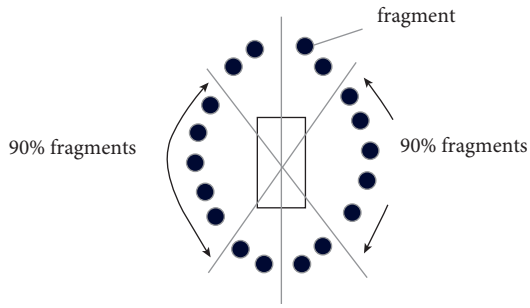


Figure 2: Fragment dispersion distribution laws.

expansion velocity upon the shell break of the fragment warhead, namely, the dispersion velocity upon the formation of fragments is defined as the initial velocity $v_0$ of the fragment. After the complete shell break, a certain further acceleration effect still exists, while the duration for the fragments being accelerated to the maximum velocity is very short. Afterwards, due to the effects of air resistance, the fragment velocity is gradually attenuated. After fragments obtain the initial velocity and get free from the effects of detonation products, they fly in air. Then, they are subject to the effects of two forces, namely, gravity and air resistance. Due to the effects of the gravity, the bending occurs to the flight trajectory of the fragment; the velocity attenuation of the fragment is caused by the air resistance. Due to the short distance and duration of the fragment flight to the target, the gravity effect may be neglected and the fragment trajectory may be approximately considered as a straight line.

Based on the basic theory of terminal effects [18], the movement differential equation of the fragment dispersion in the air may be expressed as follows:

$$m\frac{\mathrm{d}v}{\mathrm{d}t} = -\frac{1}{2}C_D\rho_a S v^2. \tag{1}$$

In equation (1), $C_D$ refers to the aerodynamic drag coefficient; $\rho_a$ refers to the air density; $S$ refers to the windward display area of the fragment; $m$, $v$, and $t$ refer to the mass, velocity and dispersion time of the fragment, respectively. The differential form between the velocity $v$ and the distance $x$ may be concluded through the conversion to the above equation:

$$m\frac{\mathrm{d}v}{\mathrm{d}x} = -\frac{1}{2}C_D\rho_a S v. \tag{2}$$

The relation between the remaining velocity of fragment dispersion and the initial velocity of fragment dispersion may be obtained through the integral conversion to equation (2):

$$v_x = v_0 e^{-(C_D\rho_a S/2m)x}. \tag{3}$$

In equation (3), $v_x$ refers to the remaining velocity of the fragment, namely, the velocity when the fragment flies to a location that is at a distance of $x$ away from the blasting center. Let

$$\alpha = \frac{C_D\rho_a S}{2m}. \tag{4}$$

Then, equation (4) may be expressed as the existing velocity equation form of the fragment:

$$v_x = v_0 e^{-\alpha x}. \tag{5}$$

In equation (5), $\alpha$ refers to the velocity attenuation coefficient of the fragment, its dimension is $m^{-1}$, and $\alpha$ represents the capacity of fragment keeping its velocity during the dispersion process; the greater $\alpha$ is, the smaller the capacity of fragment keeping its velocity is, and the faster the velocity loss is; conversely, the smaller $\alpha$ is, the greater the capacity of fragment keeping its velocity is, and the slower the velocity loss is. After the remaining velocity equation of the fragment is obtained, the scientific estimate may be made to the movement characteristics of fragment dispersion.

Introduce the unit time quantum $t$. Within the very short unit time $t$, the fragment tends towards an uniform movement, namely, $x_t = v_t \times t$. Then, it is possible to obtain the relationship between movement and time.

$$v_x = v_0 e^{-\alpha\sum_{i=0}^{x-1} v_i t}. \tag{6}$$

Hence, based on the dispersion time and initial velocity of the fragment, it is possible to compute the current remaining velocity of the fragment. According to the law that the fragment may tend towards a uniform movement within a very short unit time, it is possible to deduce the

displacement of the fragment within every unit time. Then, the three-axis coordinates can be obtained. In Figure 3, we present the coordinates and velocity of a certain reference fragment at each time snapshot.

According to the computational results, the blasting process of warhead can be simulated with the finite element simulation technology, facilitating the study on the fragment tracking algorithm.

## 3. Multitarget VPDA Algorithm

In classical data association algorithms, the essential difference between JPDA algorithm and PDA algorithm is the difference of association probability assignment ratio at which measurement values in the crossing associated gate belong to various targets. When the associated gates of various targets are crossed with each other, and the public measurement values exist in the associated gates, the assignment ratio of actual measurement values in JPDA algorithm will exceed that in PDA algorithm. Therefore, after the filtering of JPDA algorithm, the state estimate of the target is more accurate. However, due to the complexity of its association probability computation, it becomes the major reason for restricting the real-time requirements of this method. In the PDA algorithm, the probability of a measurement value within the crossing gate belonging to various targets is mutually independent. According to the first assumption of JPDA algorithm, an arbitrary measurement value must have a sole source, i.e., the measurement value must come from a target or a clutter, that is, the indiscernibility of the measurement value is not considered. The sum of probabilities of such measurement belonging to various targets will not exceed 1 (the measurement value may also come from the clutter). It is required to reconstruct a flight trajectory and the associated gates of such flight trajectory include such measurement value. The probability that such measurement value belongs to this new flight trajectory may be computed with the PDA algorithm (such probability exceeds zero). Hence, it may be concluded that the sum of probabilities of such measurement value coming from various targets will increase. With the construction of more and more new virtual flight trajectories, and the sum of probabilities of such measurement value belonging to various targets will exceed 1, inconsistent with the first assumption of the JPDA algorithm, which represents that the assignment of the probability of such measurement value within the crossing gate belonging to various targets with the PDA algorithm is unreasonable.

In order to combine the rapidity of the PDA method and the rationality of measurement value probability assignment within the crossing gate with the JPDA method, Zhao et al. [19] propose an improved fast association algorithm named as multidimensional probabilistic data association (MPDA) algorithm, which mainly considers the impact of public measurement values within the crossing gate upon the state value update of various targets.

Assume that the probability that the $j^{\text{th}}$ measurement value computed with the PDA algorithm is associated with target $t$ is $\beta_j^t(k)$. Where, $\beta_0^t(k)$ represents the probability that all measurement values are false alarms for target $t$. Then, the nature of the probability is as follows:

$$\sum_{j=0}^{m_k} \beta_j^t(k) = 1. \tag{7}$$

The probability that the distribution of $m_k$ measurement values obtained through the computation with the PDA algorithm belongs to various targets, will be constructed as the $(m_k + 1, T)$ dimensional probabilistic data association matrix $P$:

$$P = \overbrace{\begin{bmatrix} p_{01} & \cdots & p_{0T} \\ \vdots & \cdots & \vdots \\ p_{m_k 1} & \cdots & P_{m_k T} \end{bmatrix}}^{t} j, \quad j = 0, 1, \ldots, m_k, t = 1, \ldots, T, \tag{8}$$

where, $p_{jt} = \beta_j^t(k)$. Each line of the matrix $P$ is normalized to obtain the correction matrix $M$ as follows:

$$M_{jt} = \frac{p_{jt}}{\sum_{t=1}^{T} p_{jt}} \quad j = 0, 1, \ldots, m_k. \tag{9}$$

A measurement value may fall in multiple associated gates. In this case, the association probability of public measurement values assignment of crossing gates shall be subject to the weighted correction. Therefore, each line must be normalized. If a measurement value only falls in one associated gate at most, the association probability of the target corresponding to the gate where such measurement value is located does not change after the normalization. When such measurement value simultaneously belongs to multiple targets, the sum of its association probabilities may exceed 1. After the normalization, the impact of such measurement value upon the association probability of the target to which it belongs is reduced.

Obviously, after the normalization, the sum of probabilities of each line of correction matrix is not equal to 1, which destroys the criterion that the sum of association probabilities of measurement values within the associated gates and targets is equal to 1 (including the probabilities that all measurements are clutters). Each column of the correction matrix $M$ is then normalized to obtain the final probability matrix $Q$ with the MPDA method as follows:

$$Q_{jt} = \frac{M_{jt}}{\sum_{j=0}^{m_k} M_{jt}}. \tag{10}$$

The state value update method of each target is the same as PDA algorithm, but only the association probability of each measurement value and target changes. Therefore, MPDA algorithm has the computational amount approximating to that of PDA algorithm, but it also simultaneously has the association success rate and state value update error approximating to the performance of JPDA algorithm.

Based on the MPDA method, this paper proposes the VPDA algorithm based on the Doppler velocity information of blasting fragment movement characteristics model. This

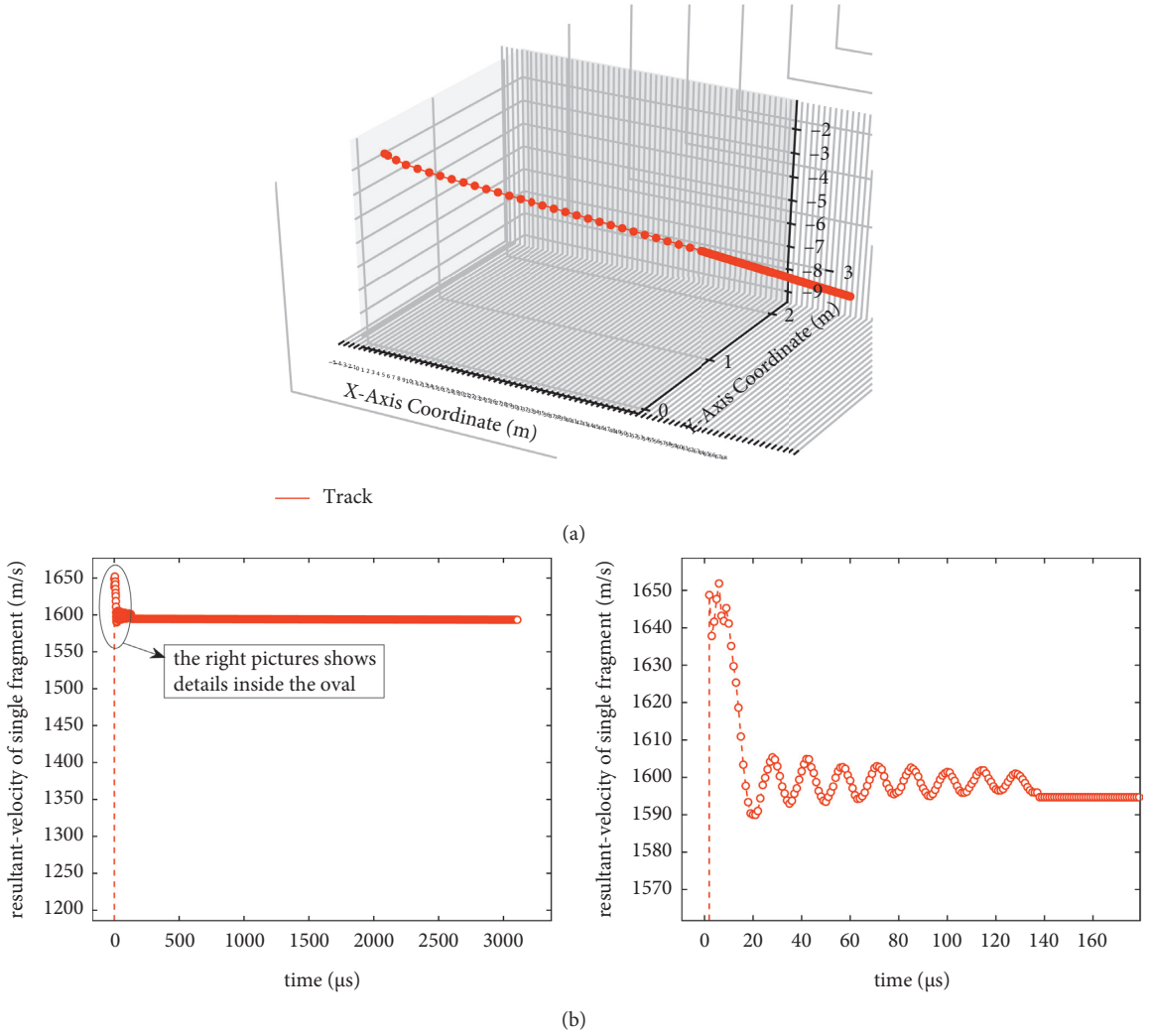


FIGURE 3: Coordinates and velocity of a certain reference fragment at each time snapshot. (a) The $X$-$Y$ coordinates of a reference fragment at each time snapshot. (b) The velocity of a reference fragment at each time snapshot.

method utilizes the advantage of MPDA algorithm, namely, it has the computational amount and state value update error approximating to those of PDA algorithm. In addition, it fully utilizes the blasting fragment movement characteristics, and further optimizes the probabilistic association matrix in the MPDA algorithm, obtaining the fragment target data association method that is applicable to the fragment with the approximate velocity within the single fragment group and also has multiple fragment groups. Through the simulation verification, this method greatly improves the high velocity multitarget association success rate and tracking precision. This method is explained in details as follows:

When the association probability of the $i^{\text{th}}$ measurement value and target $t$, the computation equation of $\beta_i(k)$ in the PDA algorithm is as shown below:

$$\begin{aligned}\beta_i(k) &= P\left\{\theta_i \mid Z(k), m_k, Z^{k-1}\right\} \\ &= \frac{p\left[Z(k) \mid \theta_i(k), Z^{k-1}\right] P\left\{\theta_i \mid m_k, Z^{k-1}\right\}}{\sum_{j=0}^{m_k} p\left[Z(k) \mid \theta_j(k), Z^{k-1}\right] P\left\{\theta_j(k) \mid m_k, Z^{k-1}\right\}},\end{aligned} \tag{11}$$

where, $Z(k)$ refers to the set of all measurement values within the associated gate at the time point $k$, i.e., $Z(k) = \{z_i(k)\}_{j=1}^{m_k}$; $\beta_i(k)$ refers to the conditional probability that the $i^{\text{th}}$ measurement value $z_i(k)$ comes from the true target, and $\beta_0(k)$ represents that all measurement values are false alarm points. $Z^{k-1}$ refers to the sum of all confirmed measurement values from the start time to the time point $k-1$, and $m_k$ refers to the sum of all measurement values within the associated gate at the time point $k$; $\theta_i$ refers to the event assumption, as defined below:

(i) $\theta_i(k) = \{z_i(k)$ is the measurement value coming from the true target$\}$, $i = 1, 2, \ldots, m_k$

(ii) $\theta_0(k) = \{$All measurement values are false alarm points$\}$

Then, introduce the fragment group's Doppler velocity probability concept. Let $p_i^{vr}(k)$ represents the association probability of the $i^{\text{th}}$ measurement value and the target, when only the overall Doppler velocity information of the fragment group with the approximate velocity is considered at the time point $k$. $p_0^{vr}(k)$ refers to the Doppler velocity probability corresponding to event $\theta_0$, and $p_0^{vr}(k) = 1$.

The computation equation of association probability can be deduced with the PDA method:

$$\beta_0(k) = \frac{b}{b + \sum_{j=1}^{m_k} e_j}, \tag{12}$$

$$\beta_i(k) = \frac{e_i}{b + \sum_{j=1}^{m_k} e_j}. \tag{13}$$

After the Doppler velocity probability is added, equations (12) and (13) are converted as follows:

$$\begin{aligned} \beta_0(k) &= \frac{b}{b + \sum_{j=1}^{m_k} e_j p_j^{vr}}, \\ \beta_i(k) &= \frac{e_i p_i^{vr}}{b + \sum_{j=1}^{m_k} e_j p_j^{vr}}. \end{aligned} \tag{14}$$

The Doppler velocity probability is computed based on the fragment movement characteristics model. Taking the 2D rectangular coordinate system (the measurement value of the target is $(x, y)$) as example, the state vector of the target at the time point $k$ is as shown below:

$$X(k) = \begin{bmatrix} x_k \\ \dot{x}_k \\ y_k \\ \dot{y}_k \end{bmatrix}. \tag{15}$$

In equation (15), $\dot{x}_k$ represents the first-order derivative of $x_k$, i.e., the velocity in the direction of $x$, and $\dot{y}_k$ represents the first-order derivative of $y$, i.e., the velocity in the direction of $y$.

Then, the Doppler velocity of the target can be expressed as follows:

$$v_r(k) = \frac{\dot{x}_k \cdot x_k + \dot{y}_k \cdot y_k}{\sqrt{x_k^2 + y_k^2}}. \tag{16}$$

When the Doppler velocity function of the target is expanded at the target state value by utilizing the Taylor's series, it is converted as follows:

$$v_r(k) = \begin{bmatrix} \frac{\partial v_r(k)}{\partial x_k} & \frac{\partial v_r(k)}{\partial \dot{x}_k} & \frac{\partial v_r(k)}{\partial y_k} & \frac{\partial v_r(k)}{\partial \dot{y}_k} \end{bmatrix} \begin{bmatrix} x_k \\ \dot{x}_k \\ y_k \\ \dot{y}_k \end{bmatrix}. \tag{17}$$

When the partial derivatives are taken with equation (16), the following first-order partial derivatives at various state values of the target are obtained respectively for the Doppler velocity function:

$$\begin{aligned} \frac{\partial v_r(k)}{\partial x_k} &= \frac{\dot{x}_k \cdot y_k^2 - x_k \cdot y_k \cdot \dot{y}_k}{\left(x_k^2 + y_k^2\right)^{3/2}}, \\ \frac{\partial v_r(k)}{\partial \dot{x}_k} &= \frac{x_k}{\sqrt{x_k^2 + y_k^2}}, \\ \frac{\partial v_r(k)}{\partial y_k} &= \frac{\dot{y}_k \cdot x_k^2 - x_k \cdot y_k \cdot \dot{x}_k}{\left(x_k^2 + y_k^2\right)^{3/2}}, \\ \frac{\partial v_r(k)}{\partial \dot{y}_k} &= \frac{y_k}{\sqrt{x_k^2 + y_k^2}}. \end{aligned} \tag{18}$$

Let $H_{vr}(k) = [\ (\partial v_r(k)/\partial x_k)\ \ (\partial v_r(k)/\partial \dot{x}_k)\ \ (\partial v_r(k)/\partial y_k)(\partial v_r(k)/\partial \dot{y}_k)]$ and add the Doppler velocity measurement error. Then, it is expressed as follows:

$$v_r(k) = H_{vr}(k) \cdot X(k) + w_{vr}. \tag{19}$$

Assume that the Doppler velocity of the clutter conforms to the even distribution conditions in the Doppler velocity measurement space, and the Doppler velocity measurement value of the target satisfies the Gaussian distribution. Then, $w_{vr}$ represents that the mean value is zero and the standard difference is the Gaussian random variable of $\sigma_{vr}$. The following target's predicted value of Doppler velocity at the current time point is obtained from the target's predicted state value $X(k \mid k-1)$ at the current time point:

$$v_r(k \mid k-1) = H_{vr}(k) \cdot X(k \mid k-1). \tag{20}$$

The Doppler velocity innovation covariance is as follows:

$$S_{vr}(k) = H_{vr}(k) P(k \mid k-1) H_{vr}'(k) + \sigma_{vr}^2, \tag{21}$$

where, $P(k \mid k-1)$ refers to the predicted value of target state value error covariance.

Then, assume that the Doppler velocity of the $i^{\text{th}}$ measurement value at the time point $k$ is $v_r^i(k)$, the Doppler velocity innovation is expressed as follows:

$$v_{vr}^i(k) = v_r^i(k) - v_r(k \mid k-1). \tag{22}$$

Hence, the following Doppler velocity probability $p_i^{vr}(k)$ is obtained:

$$p_i^{vr}(k) = \frac{1}{\sqrt{2\pi S_{vr}(k)}} e^{-\left( \left(v_{vr}^i(k)\right)^2 / 2\sigma_{vr} \right)}. \quad (23)$$

After the Doppler velocity probability is obtained, the association probability $\beta_i(k)$ in the PDA algorithm can be obtained through equation (11). Finally, the association probability is updated according to the above MPDA algorithm, which is the computation procedure of Doppler velocity-based VPDA algorithm.

Generally, the computational amount of JPDA algorithm grows exponentially with the number of targets and the number of measurement values, and the computational amount of PDA algorithm grows linearly with the number of targets and the number of measurement values. Based on the MPDA algorithm, this paper proposes the VPDA method through verification, and only the Doppler velocity probability is utilized to reassign the association probability. The complexity of its algorithm is in the same order as that of PDA algorithm. However, its complexity is far below that of JPDA algorithm and it has the superiority, when there are more targets or measurement values.

## 4. Simulation Experiment

In combination with contents described herein, this paper firstly simulates the warhead fragment dispersion, and verifies the correctness of such simulation model through a certain treatment; in addition, based on the fragment movement characteristics demonstrated by such simulation model, the epipolar multitarget tracking performance is tested for the VPDA algorithm proposed herein.

*4.1. Simulation of Blasting Fragment Movement Characteristics.* The finite element simulation involved herein utilizes the TrueGrid software for modeling and preprocessing works, and the LS-DYNA software is utilized to carry out the computation, solving and postprocessing for the model. Select the large-caliber blast-fragmentation grenade weapon as the study object, and the warhead entity model is simplified during the modeling process. Neglect the shooting head and detonation propagation part, and convert the projectile body warhead into the cylindrical structure. Model the warhead as a cylinder structure and assume the outer diameter of warhead as 70 mm and shell wall thickness as 5 mm; in addition, assume the TNT charge length as 138 mm, and the charge diameter as 60 mm. The fragments are natural fragments generated from the charge blasting shock. In this simulation, the physical situations of fragment failure under stress are described through the SPH particulate conversion method. Most of the typical natural fragments generated in the simulation are 130~150 SPH particulate sets. According to the unit size and material density computation, the typical fragment mass is about 1.1 g, and the overall simulation results are as shown in Figures 4 and 5. Figure 4 shows the conditions of natural fragments generated from warhead on a top view, and Figure 5 shows the partial typical natural fragments generation conditions.

Figure 4: Conditions of natural fragments generated from warhead (warhead top view).

Figure 5: Partial typical natural fragments generation conditions (local).

Take 50 $\mu$s as the time interval, obtain the fragment dispersion process by capturing the fragment dispersion conditions of simulation model at various moments, and get the results as shown in Figure 6 by applying the effective stress in the LS-DYNA to display the model.

It is observed that after the powder blasting, the warhead swells and grows, the natural fragments are gradually detached and the overall fragment dispersion is relatively even. As shown in the effective stress indication, it is found that the simulated fragment rollover phenomenon is not obvious. As shown from the distribution colors of the effective stress, it is found that the stress of fragments approaching to both ends is much lower, the lower fragment velocity is below the upper fragment velocity, and the stress in the middle part is the highest. This conforms to the basic physical laws and also explains the rationality of simulation model.

Besides, it is found that most natural fragments have already been stabilized at the velocity of about 50 $\mu$s through selection of reference fragments, and extraction of velocity, dispersion angle and other data, that, the fragment is not accelerated any more. Among all the selected fragments, the maximum velocity is 1600 m/s and the minimum velocity is 1100 m/s. The velocity of selected fragments is concentrated at 1350 m/s. The dispersion direction of the natural fragments generated from the shell is concentrated at the angle of about 85.5°. Subject to the end effects, the distribution of the square fragments at both ends of the warhead is much more discrete, namely, the fragment density at the dispersion edge is much lower.

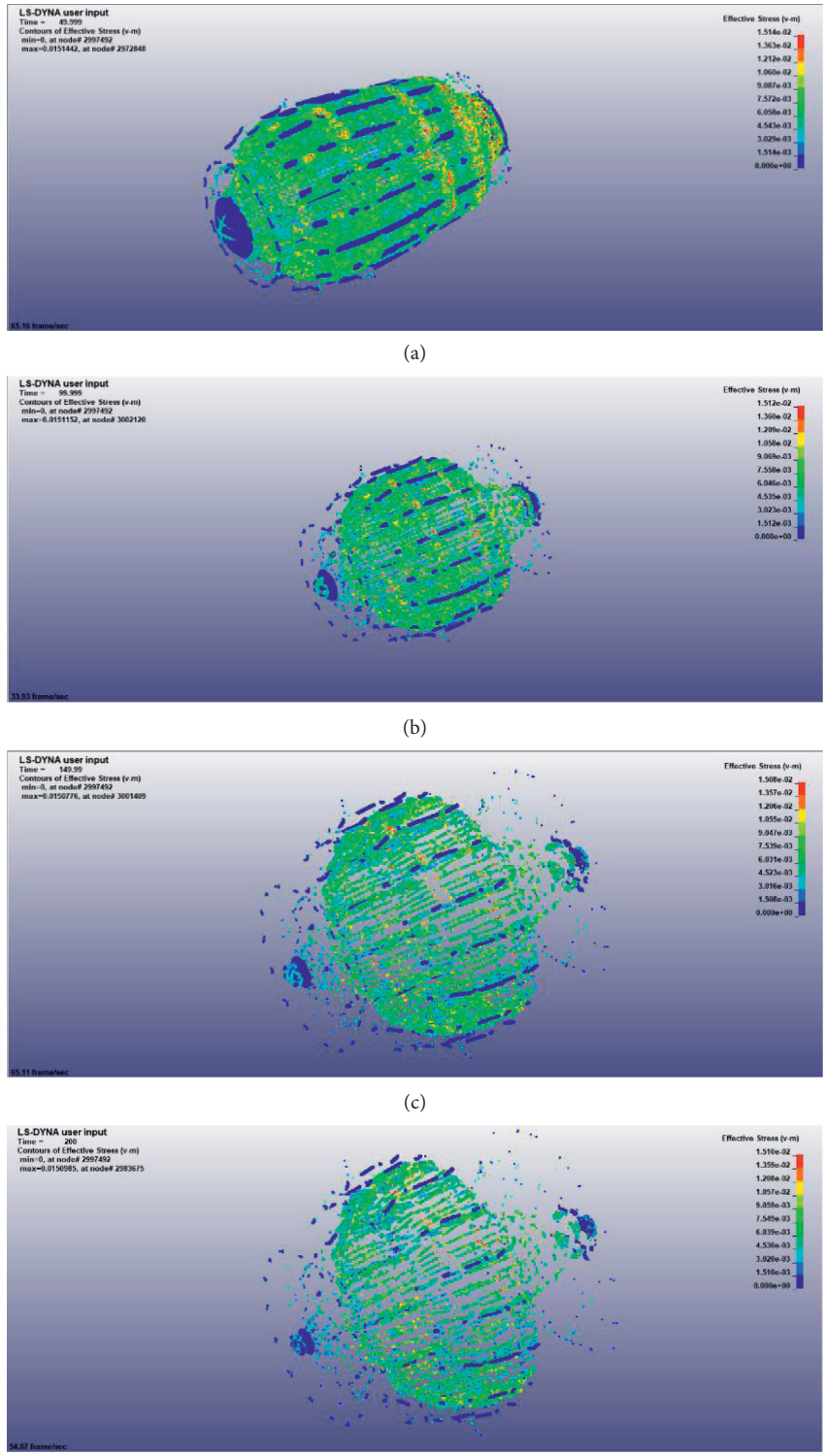


Figure 6: Simulation of fragment dispersion conditions. (a) $t = 50\,\mu$s. (b) $t = 100\,\mu$s. (c) $t = 150\,\mu$s. (d) $t = 100\,\mu$s.

*4.2. Performance Simulation Experiment of VPDA Algorithm.* The performance simulation verification of the VPDA algorithm consists of two experiments. In the first experiment, the fastness and precision of VPDA algorithm is verified through the comparison of the multitarget data association processing effects with the PDA algorithm, JPDA algorithm and VPDA algorithm; in the second experiment, the warhead flight and blasting process is simulated, further verifying the practicability of VPDA in the small-scale blasting fragment scenario.

*4.2.1. Simulation Experiment 1.* In order to compare the multitarget data association processing effects with the PDA algorithm, JPDA algorithm and VPDA algorithm, set two real targets with the movement state of uniform linear movement, initial state values (position in the direction of $x$, velocity in the direction of $x$, position in the direction of $y$, and the velocity in the direction of $y$) of (400, 20, 600,10) and (600, 10, 100, 20) separately, target position in $m$ and velocity in m/s. The simulation step size is 80 frames, and the probability that the actual measurement value falls in the associated gate is $P_G = 0.99$. When the number of clutters within the area of 1 km$^2$ is 1000, the data association results with the three methods are as shown.

The association results of the above three methods are shown in Figures 7–9. In Figure 7, trajectory merging occurs to the PDA algorithm after frame 40, which causes tracking error and subsequently deteriorates the positioning performance. From the comparison results in Figures 8 and 9 we may find that both JPDA algorithm and VPDA algorithm can accurately achieve data association and realize target tracking. In addition, the positioning errors are very close to each other, as shown in Figures 10 and 11.

As to the computational complexity, 1000 Monte-Carlo experiments are performed in this paper. The average computation time of processing the 80-frame data is 0.5362 s for JPDA algorithm, which is 0.0417 s for VPDA algorithm. Therefore, the VPDA algorithm based on the Doppler velocity has similar data association performance with the JPDA, but the computational cost is much less than that of JPDA algorithm. The amount is very close to the well-known PDA algorithm, which is 0.0388 s.

In addition, different number of targets are simulated to demonstrate the computational advantage of the proposed VPDA algorithm. Four scenarios with 2/4/6/8 targets are processed using the above three algorithms. 1000 Monte-Carlo experiments are also performed for each scenario and the experiment conditions are maintained. Computer configurations are i7-8700K CPU, NVIDIA RTX-2070 GPU, and 16 GB RAM. Figure 12 plots the average computation time of each algorithm.

It can be seen from Figure 12, the average computation time increases with number of targets for all algorithms. However, the JPDA has a higher increasing rate, which costs too much time for dense target scenario. In our applications, the number of fragments may reach several thousand. Therefore, the JPDA algorithm could not be applied. The computational complexity of the proposed VPDA algorithm is a little higher than that of PDA algorithm. Both methods show much slower increasing rate. Considering the PDA algorithm is not suitable for multitarget tracking, we may get the conclusion that the VPDA algorithm achieves a better balance between tracking performance and computational complexity.

*4.2.2. Simulation Experiment 2.* In order to verify the tracking performance of VPDA algorithm upon the blasting fragment target, it is required to simulate the whole flight and blasting process of the warhead. Assume that the

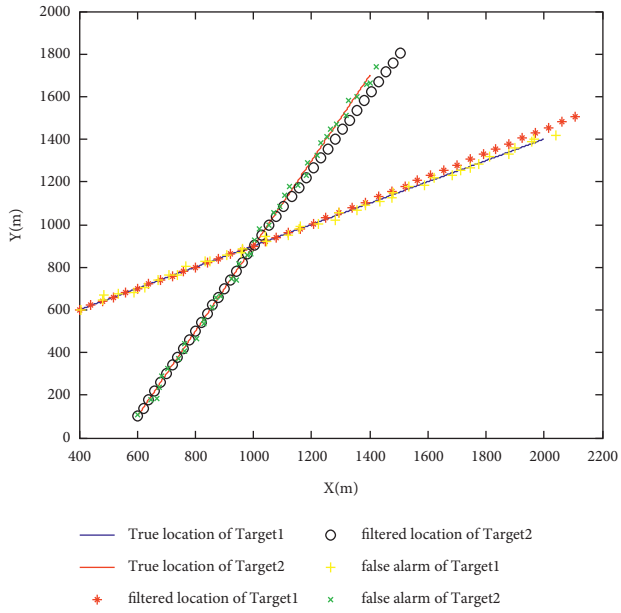


Figure 7: PDA association results.

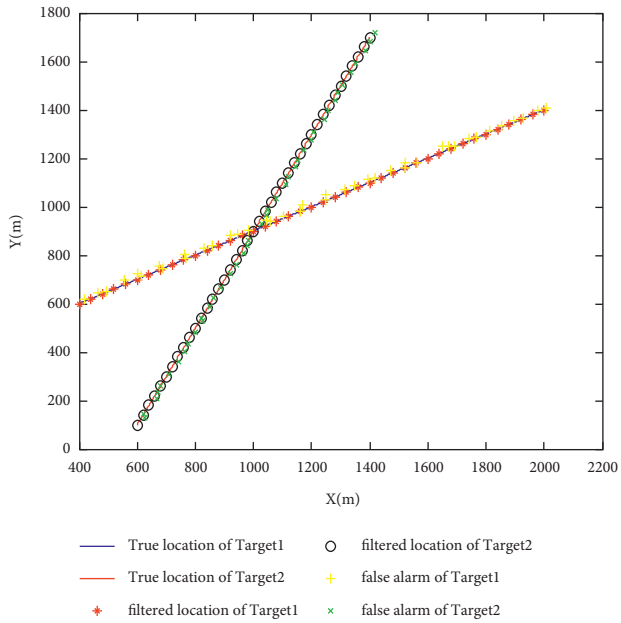


Figure 8: JPDA association results.

resistance in the flight process of a warhead is in direct proportion to the square of velocity, and the direction is opposite to the velocity direction. The resistance to the missile at the initial time point is twice of its weight. In addition, during the flight process, the artillery shell is also subject to the zero-mean white noise disturbing force in the directions of $x$, $y$ and $z$, enabling the artillery shell to arbitrarily obtain the force with the variance of $1N$ in the directions of $x$, $y$ and $z$. Due to the impact effect generated from the blasting, not only the 11 target fragments blasted, released and carried at a given time point, have the initial velocity of warhead, but also the warhead obtains the fragment group distribution and initial velocity during the

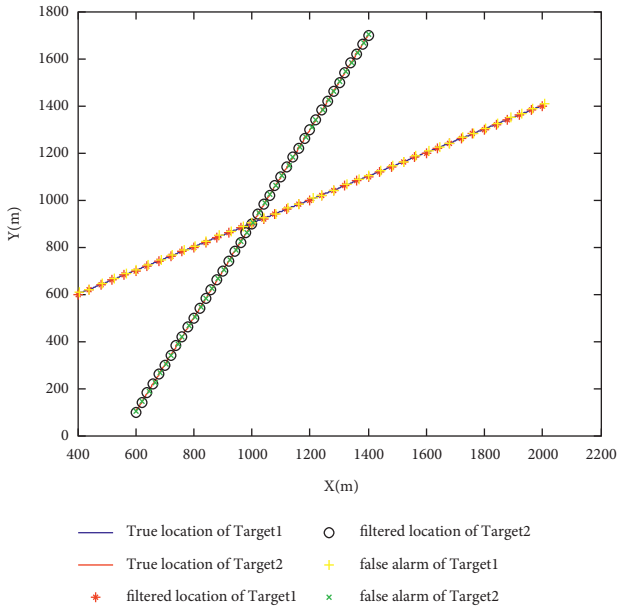


Figure 9: VPDA association results.

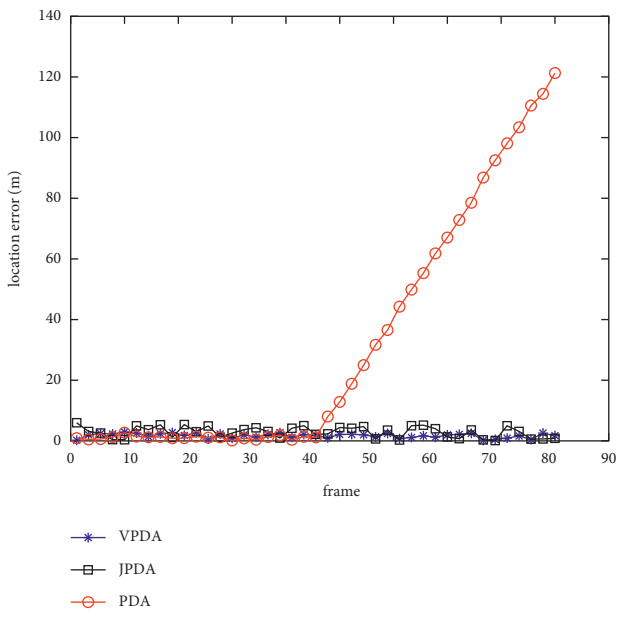


Figure 10: Target 1 positioning errors.

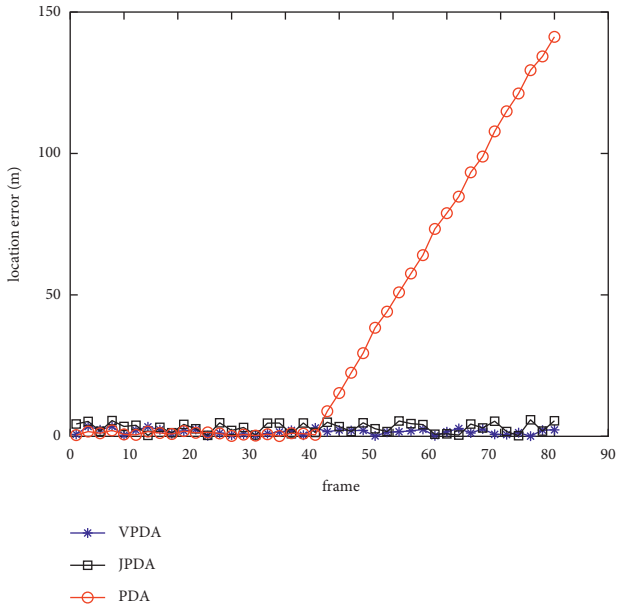


Figure 11: Target 2 positioning errors.

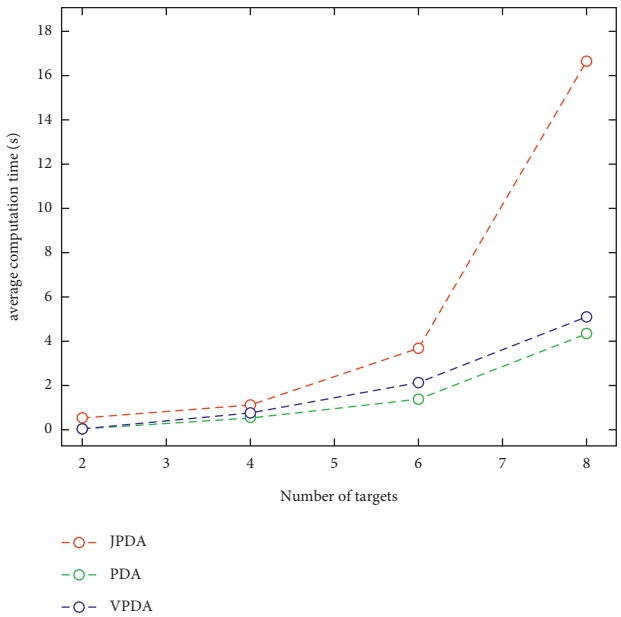


Figure 12: The average computation of three algorithms with different number of targets.

simulation process as shown in Section 3 in the directions of $x$, $y$ and $z$, and the fragments occur to the cube in the coordinates of $x \pm 50$, $y \pm 50$ and $z \pm 50$ nearby the blasting pointing $(x, y, z)$.

The whole-process real-time tracking is made to the warhead and fragments with the algorithm proposed herein and the sensor is located at $(r_x, r_y, r_z)$. The range error is 10 m and both the angle (azimuth angle and pitch angle) measurement errors are 0.1°. The range error and angle measurement errors are subject to the zero-mean Gaussian white noise distribution and the sampling frequency is 200 Hz. The clutters are evenly distributed within the survey space. The number of clutters is subject to the Poisson distribution, and the density is $1 \times 10^{-8}$ nos./m$^3$. After modeling of the system, the real-time tracking effects are obtained with the VPDA algorithm proposed herein, as shown in Figure 13.

The different colors of lines as shown in the above figure represent the actual movement trajectory of variable targets, that is, 12 targets in total. The "+" symbol represents the estimated position of the target after filtering. It is found that the movement process of the targets is divided into two phases. Among them, there is only one target in phase 1, the movement model is similar to the projectile movement, and the tracking is precise; the targets in phase 2 are generated

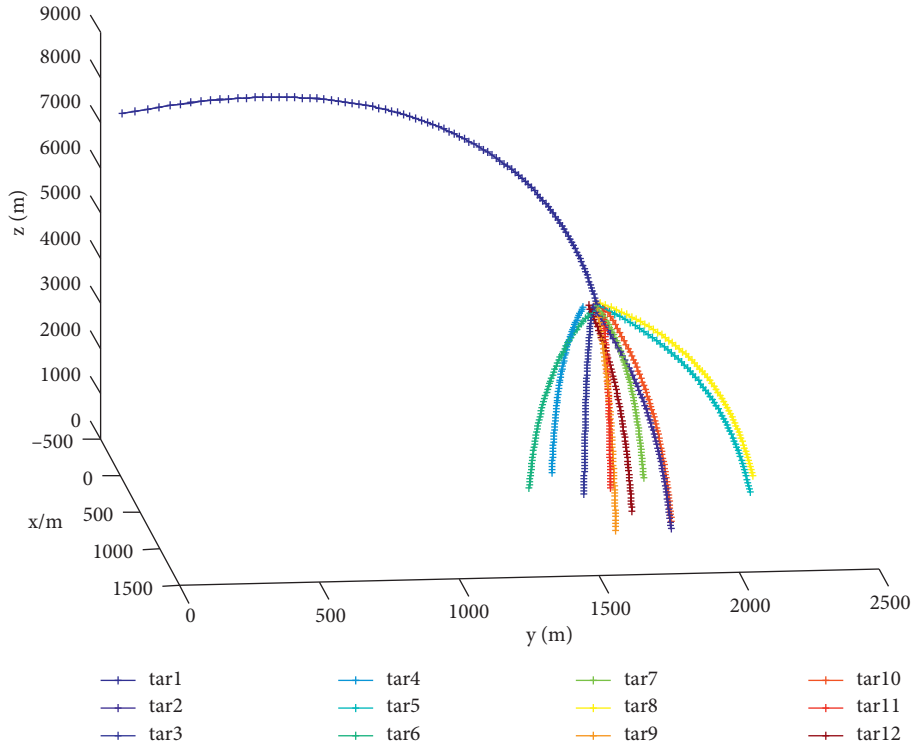


Figure 13: 12-target concurrent tracking effects.

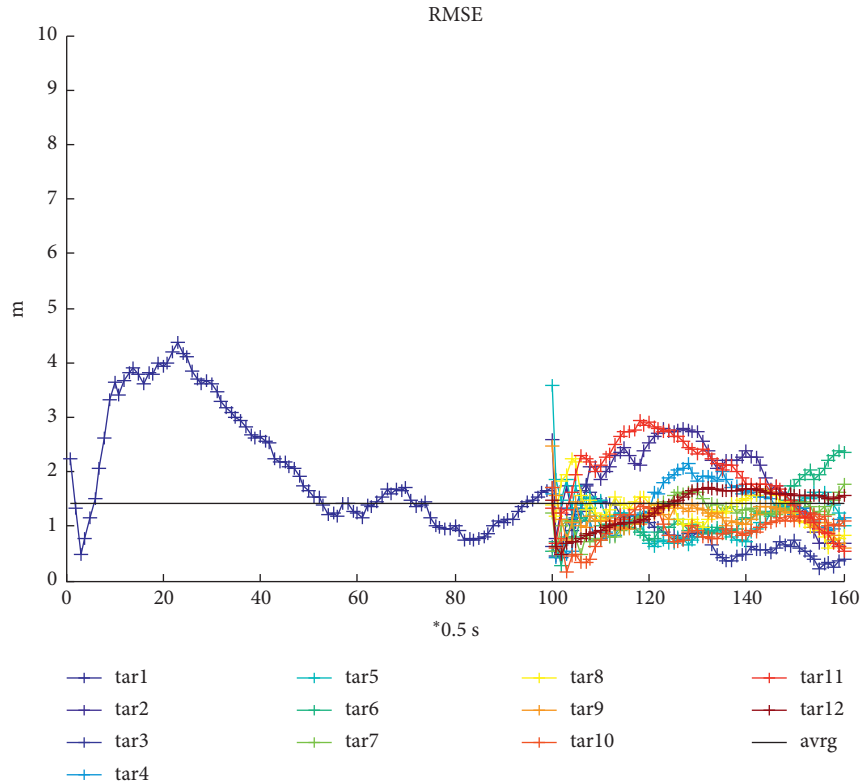


Figure 14: Filtering root-mean-square error of 12 targets being tracked.

from the blasting of the target in phase 1, that is, there are 11 targets in phase 2. In addition, the velocities, sizes and directions vary, but the movement models are similar, namely, all of them are non-maneuvering movement models. Due to the number sharp increase of the targets, the dimension of the confirmed matrix is increased to at least $m_k \times 12$. As a result, in the most ideal case, the number of feasible events is $2^{11} = 2048$ (11 measurement values separately fall into the non-overlapping gate zone of 11 targets). Therefore, the impact of the number of targets upon the number of feasible events is exponential. As a result, the modified $K$-means-clustering-based algorithm proposed herein is adopted to reduce the dimension of the confirmed matrix. As shown in the tracking effect figure in phase 2, no tracking loss or defect tracking occurs to the 11 targets and the tracking effects are good.

The filtering root-mean-square error and the global root-mean-square error are as shown in Figure 14:

As shown in Figure 14, the filtering root-mean-square error $\mathrm{RMSE}_{xyz}(j)$, $j \in [1, 101]$, $j \in N$ in the flight of warhead in phase 1 tends to be stable, when $j$ is about 40; the filtering root-mean-square error becomes larger at the initial blasting time point in phase 2. Afterwards, certain fluctuations occur and then it is gradually stabilized below 3 m. The global root-mean-square error RMSE is 1.4158 m, and compared with the measurement precision it is greatly improved. Therefore, the algorithm proposed herein conforms to the requirements in terms of the tracking precision.

The movement characteristics model of blasting fragments is used during the flight trajectory association and target tracking process. Although the number of feasible event targets declines sharply, it almost conforms to the real-time tracking requirements, and the filtering precision also conforms to the requirements, which indicate that the VPDA algorithm proposed herein can be applied to the group target tracking field.

In practice, the number of warhead fragments can reach thousands of scales, such a large scale number is invalid with the traditional multitarget tracking algorithm. In the work done of our paper, the numerical simulation shows that there is a strong correlation between the trajectories of fragments near the position, therefore, in the actual algorithm processing, according to the fragment movement characteristic and the trajectory carries on the cluster processing then uses the multitarget tracking algorithm, after this clustering, the target point corresponds to the real many small fragments which composed the fragment group.

## 5. Conclusions

This paper proposes the Doppler velocity-based multitarget VPDA algorithm. In order to verify the performance of this algorithm, the finite element simulation technology is utilized to establish the warhead blasting fragment dispersion model. Based on the dispersion fragment movement characteristics demonstrated by this model, two simulation experiments are designed and the computational amount, accuracy and applicability of the VPDA algorithm are verified. As shown from the simulation results, the VPDA algorithm fully utilizes the Doppler information of the blasting fragment target, which not only overcomes the trajectory merging problem easily occurring upon the processing of multitarget association with the PDA algorithm, but also combines the processing idea of JPDA algorithm for the measurement value within the crossing gate. Its computational amount is approximate to that of PDA algorithm, its association success rate and the state value update error are approximate to the association effect of JPDA algorithm, and it can respond to the group target tracking scenario.

## Data Availability

The simulation data implemented on MATLAB used to support the findings of this study are available from the corresponding author upon request.

## Conflicts of Interest

The authors declare that they have no conflicts of interest.

## Acknowledgments

This work was supported by the China Postdoctoral Fund (2017M623349).

## References

[1] W. Jinhui and L. Ji, "Development status of testing the parameters of warhead fragment in the static explosive field," *Journal of Ordnance Equipment Engineering*, vol. 40, no. 10, pp. 104–110, 2019.

[2] S. M. Holmes, "Fragment tracking-insights into what happens in explosions," Report, Sandia National Laboratories, Albuquerque, NM, USA, 2016.

[3] F. Robert and Behler, "Director, operational test and evaluation FY2019 annual report," Report, United States Department of Defense, VA, USA, 2019.

[4] J. Hou, Z. Han, X. Li et al., "Analysis and modeling of radar echo for warhead dynamic explosion fragments," *Chinese Journal of Modern Electronics Technique*, vol. 38, no. 17, pp. 6–8, 2015.

[5] C. Bai, H. Wang, and F. Chun, "Analysis of criteria for assessing safety distance for focused warhead fragments based on CDEM," *Mathematical Problems in Engineering*, vol. 2019, Article ID 8735481, 12 pages, 2019.

[6] H. Li, X. Zhang, and X. Zhang, "Calculation model and method of target damage efficiency assessment based on warhead fragment dispersion," *IEEE Transactions on Instrumentation and Measurement*, vol. 70, pp. 1–8, 2020.

[7] J. Sheng, "Target identity recognition method based on RCS distribution and spatial location," *Procedia Computer Science*, vol. 147, pp. 632–637, 2019.

[8] X. Gong, L. Zichun, W. Hui et al., "Survey of data association technology in multi-target tracking," *Computer Science*, vol. 47, no. 10, pp. 136–144, 2020.

[9] Y. Barshalom, F. Daum, and J. Huang, "The probabilistic data association filter," *IEEE Control Systems Magazine*, vol. 29, no. 6, pp. 82–100, 2012.

[10] P. L. Ainsleigh, T. E. Luginbuhl, and P. K. Willett, "A sequential target existence statistic for joint probabilistic data

association," *IEEE Transactions on Aerospace and Electronic Systems*, vol. 57, no. 1, pp. 371–381, 2021.

[11] S. H. Bae and K. J. Yoon, "Robust online multiobject tracking with data association and track management," *IEEE Transactions on Image Processing*, vol. 23, no. 7, pp. 2820–2833, 2014.

[12] P. U. Damale, E. K. P. Chong, and T. J. Ma, "Performance study of distance-weighting approach with loopy sum-product algorithm for multi-object tracking in clutter," *Sensors*, vol. 21, no. 7, p. 2544, 2021.

[13] L. Sun, Y. Cao, W. Wu et al., "A multi-target tracking algorithm based on gaussian mixture model," *Journal of Systems Engineering and Electronics*, vol. 31, no. 3, pp. 482–487, 2020.

[14] Y. Guo, Y. Li, A. Xue, R. Tharmarasa, and T. Kirubarajan, "Simultaneous tracking of a maneuvering ship and its wake using gaussian processes," *Signal Processing*, vol. 172, Article ID 107547, 2020.

[15] Y. Likui and J. Jianwei, "Calculation model of initial velocity field on multilayered spherical fragments warhead," *Chinese Journal of Energetic Materials*, vol. 22, no. 3, pp. 300–305, 2014.

[16] W. Hongbo, W. Xiaohan, and K. Li, "Analysis of dispersion movement rule of warhead fragment for ship-air missile," *Ship Electronic Engineering*, vol. 5, pp. 40–42+76, 2012.

[17] H. Yutao, J. Banghai, L. Fangyun et al., "Simulation of fragment warhead attack based on LS-DYNA simulation results," *Journal of Ballistics*, vol. 24, no. 1, pp. 27–31, 2012.

[18] S. Shuyuan, *Terminal Effects*, National Defense Industry Press, Beijing, China, 2000.

[19] Y. Zhao, H. Lin, F. Zhao et al., "Data association and track management in multitarget tracking," *Chinese Journal of Modern Radar*, vol. 29, no. 3, pp. 28–31, 2007.